Naval Research Laboratory

Washington, DC 20375-5000

AD-A242 433

91-15196

Analysis of the Deflection System for a Magnetic-Field-Immersed Magnicon Amplifier

B. HAFIZI,[*] Y. SEO,[**] S. H. GOLD, W. M. MANHEIMER AND P. SPRANGLE

Beam Physics Branch
Plasma Physics Division

[*]Icarus Research
7113 Exfair Rd.
Bethesda, MD 20814

[**]FM Technologies, Inc.
Fairfax, VA 22032

November 5, 1991

REPORT DOCUMENTATION PAGE

Public reporting burden for this collection of information is estimated to average 1 hour per response, including the time for reviewing instructions, searching existing data sources, gathering and maintaining the data needed, and completing and reviewing the collection of information. Send comments regarding this burden estimate or any other aspect of this collection of information, including suggestions for reducing this burden, to Washington Headquarters Services, Directorate for Information Operations and Reports, 1215 Jefferson Davis Highway, Suite 1204, Arlington, VA 22202-4302, and to the Office of Management and Budget, Paperwork Reduction Project (0704-0188), Washington, DC 20503

1. AGENCY USE ONLY (Leave blank)	2. REPORT DATE	3. REPORT TYPE AND DATES COVERED
	1991 November 5	Interim

4. TITLE AND SUBTITLE

Analysis of the Deflection System for a Magnetic-Field-Immersed Magnicon Amplifier

5. FUNDING NUMBERS

J.O. #47-3788-01

6. AUTHOR(S)

B. Hafizi,* Y. Seo,** S. H. Gold, W. M. Manheimer and P. Sprangle

7. PERFORMING ORGANIZATION NAME(S) AND ADDRESS(ES)

Naval Research Laboratory
Washington, DC 20375-5000

8. PERFORMING ORGANIZATION REPORT NUMBER

NRL Memorandum
Report 6793

9. SPONSORING/MONITORING AGENCY NAME(S) AND ADDRESS(ES)

U.S. Department of Energy
Washington, DC 20545

Office of Naval Research
Arlington, VA 20545

10. SPONSORING/MONITORING AGENCY REPORT NUMBER

11. SUPPLEMENTARY NOTES

*Icarus Research, 7113 Exfair Rd., Bethesda, MD 20814
**FM Technologies, Inc., Fairfax, VA 22032

12a. DISTRIBUTION/AVAILABILITY STATEMENT

Approved for public release; distribution unlimited.

12b. DISTRIBUTION CODE

13. ABSTRACT (Maximum 200 words)

A linear analysis of the electron beam deflection system in a magnicon is presented. The system consists of identical cavities, one driven and the remainder passive, separated by a drift space, and immersed in an axial magnetic field. The cavities contain a rotating TM_{110} mode. The length of each cavity is $\pi v_z/\omega$ and that of the drift space is $\pi v_z/\omega_c$, where ω is the rf frequency, ω_c is the relativistic gyrofrequency in the guide field and v_z is the mean axial velocity of the beam electrons. The linearized electron orbits are obtained for arbitrary initial axial velocity, radial coordinate and magnetic field. The small-signal gain and the phase shift are determined. The special case where $\omega_c/\omega = 2$ has unique features and is discussed in detail. For example, this special case gives rise to a constant phase of the electrons relative to that of the TM_{110} mode and the passive cavity may be driven optimally for a given beam current. For the NRL magnicon design, a power gain of 10 dB per passive cavity is feasible. Operation of the output cavity at the fundamental and higher harmonics of the input drive frequency is briefly discussed.

14. SUBJECT TERMS		15. NUMBER OF PAGES
Magnicon	Driven and Passive Cavities	28
Deflection System	Gain and Phase Shift	**16. PRICE CODE**

17. SECURITY CLASSIFICATION OF REPORT	18. SECURITY CLASSIFICATION OF THIS PAGE	19. SECURITY CLASSIFICATION OF ABSTRACT	20. LIMITATION OF ABSTRACT
UNCLASSIFIED	UNCLASSIFIED	UNCLASSIFIED	SAR

CONTENTS

iii

ANALYSIS OF THE DETECTION SYSTEM FOR A MAGNETIC-FIELD-IMMERSED MAGNICON AMPLIFIER

I. Introduction

The magnicon, recently proposed in the Soviet Union, employs scanning beam modulation of a moderately relativistic electron beam (typically < 1 MeV) to efficiently generate high-power microwaves with potentially diverse applications.[1] The magnicon consists of a sequence of cavities, the first of which is driven, and the remainder are passive. As a solid electron beam with small initial transverse momentum traverses the cavities, it is progressively spun up to produce a high-transverse-velocity electron beam for injection into the output cavity. The deflection cavities employ a rotating TM_{110} mode, so that the beam is coherently spun up. The point of injection of the beam into the output cavity and its instantaneous guiding center rotate about the device axis at the drive frequency. A magnicon resembles a gyroklystron amplifier in that the interaction in the output cavity takes place at the gyrofrequency and involves only the transverse beam momentum. In a gyroklystron, however, the beam transverse momentum is produced prior to its bunching cavities, and the beam is bunched in phase ballistically in the drift spaces separating the cavities, in a manner analogous to the ballistic axial bunching employed in conventional klystrons.[2] In a magnicon, there is complete modulation of the phase since the electrons are deflected transversely in a deflection system, and are injected into the unstable mode in the output cavity in phase synchronism with a rotating rf wave. Consequently the transverse efficiency may be extremely high. In a gyroklystron the phase modulation is incomplete and a fraction of the electrons are actually accelerated by the rf electric field of the output cavity. Because of the need for a deflection system, a magnicon can be operated only as an amplifier.

The Soviet literature describes two different magnicon designs. The first of these generated 2 MW at 915 MHz with an efficiency of 73% as a first harmonic amplifier.[1] The second, which is in the construction phase, is designed to generate 60 MW at 7 GHz and 70% efficiency as a second harmonic amplifier.[3] At the Naval Research Laboratory (NRL) we are presently designing a high-gain, second-harmonic magnicon experiment in the X-band.[4] The design calls for the generation of 50 MW at 11.4 GHz and 50% efficiency, using a 200 A, 1/2 MV electron beam produced by a cold-cathode diode on the NRL Long-Pulse Accelerator Facility.[5]

In this paper we investigate the deflection system of a magnicon. The system is assumed to be immersed in a strong guide magnetic field so that a high perveance electron beam may be employed. The deflection system consists of an input cavity and one or more passive cavities. Each cavity contains a rotating TM_{110} mode. An input signal powers the cavity mode in the input cavity and deflects an electron beam injected close to the axis. After passing through the drift space, the electrons interact with and amplify another rotating TM_{110} mode in the passive cavity. The analysis in this paper is valid for an arbitrary ratio of the gyrofrequency to the rf frequency. However, the case where this ratio is exactly 2 has special properties and is discussed in detail. A major simplifying assumption of the analysis is that the electron energy and the axial velocity are constants in each cavity. In Sec. II we investigate the input cavity. Section III examines the passive cavities. In Sec. IV some comments on the output cavity are made and, in particular, on the operation of the output cavity at a harmonic of the drive frequency. Concluding remarks are presented in Sec. V.

II. Input Cavity

The TM_{110} mode in a cylindrical cavity may be represented by the vector potential

$$A_z = \frac{E_0 c}{i\omega} J_1(p_{11} r/a) \exp[i\phi - i\omega t] + \quad c.c. \quad , \tag{1}$$

where r, ϕ, z denote the cylindrical coordinates, E_0 is a constant, c is the speed of light, ω is the (angular) frequency, J_1 is the ordinary Bessel function of first kind of order 1, p_{11} is the first zero of J_1, a is the radius of the cavity, the cutoff wavenumber is defined by $k_c \equiv p_{11}/a = \omega/c$, and c.c. stands for complex conjugate. Figure 1 shows a cross-sectional view of the electric and magnetic field lines. The whole structure rotates azimuthally with a frequency ω, and has no z dependence within the cavity. The cavity wall radius a is determined by the boundary condition $J_1(p_{11}) = 0$. Since $p_{11} = 3.83$, the radius of the input cavity is 3.2 cm for a drive frequency of 5.7 GHz.

We shall assume that the electrons are injected along the longitudinal (z) axis of the cavity, and remain close to the axis. In the paraxial approximation, the electric and magnetic fields are given by

$$B_x = E_0 \cos \omega t \quad , \tag{2}$$

$$B_y = E_0 \sin \omega t \quad , \tag{3}$$

$$E_z = E_0(p_{11}/a)(x \cos \omega t + y \sin \omega t) \quad . \tag{4}$$

Here we use Cartesian coordinates for convenience. Electrons see a rotating transverse magnetic field with a constant amplitude E_0, and a small longitudinal electric

3

field. Transverse deflection of the electron orbit is caused by the rotating magnetic field. Imposing a constant guide magnetic field B_0, in addition to the fields (2) - (4), the beam centroid motion is governed by the following equation

$$\frac{d}{dt}v_\perp = i\omega_c v_\perp - i\omega_e v_{z0}\exp(i\omega t) \; , \tag{5}$$

where $\mathbf{v} = (v_x, v_y, v_z)$ is the velocity, $v_\perp = v_x + iv_y$, $\omega_c = |e|B_0/\gamma_0 mc$, $\omega_e = |e|E_0/\gamma_0 mc$, and e is the charge on an electron. It is assumed that the signal strength is sufficiently small and that the relativistic mass factor γ_0 and the longitudinal velocity v_{z0} of the electron under consideration may be supposed to be constants. Defining $x_\perp = x + iy$, and denoting by t_0 the initial time at which the centroid of the beamlet under consideration enters the cavity, the solution of Eq. (5) with the initial conditions $x_\perp(t = t_0) = x_{\perp 0}$ and $v_\perp(t = t_0) = v_{\perp 0}$ is

$$\begin{aligned}
x_\perp &= x_{\perp 0} - \frac{\omega_e v_{z0}}{i\omega(\omega - \omega_c)}[\exp(i\omega t) - \exp(i\omega t_0)] \\
&+ \frac{1}{i\omega_c}\left[\frac{\omega_e v_{z0}}{\omega - \omega_c}\exp(i\omega t_0) + v_{\perp 0}\right]\{\exp[i\omega_c(t - t_0)] - 1\}.
\end{aligned} \tag{6}$$

In the special case where the gyrofrequency in the guide magnetic field satisfies

$$\omega_c = 2\omega \; , \tag{7}$$

the orbit is greatly simplified.[1] In this case and for an electron starting out on the axis with no transverse velocity, i.e., with the initial conditions $x_{\perp 0} = v_{\perp 0} = 0$, Eq. (6) reduces to

$$x_\perp = -i\frac{2\omega_e v_{z0}}{\omega^2}\sin^2\frac{\theta}{2}\,\exp(i\omega t) \; , \tag{8}$$

where $\theta = \omega(t - t_0) \approx (\omega/v_{z0})z$ is the flight angle. It is to be noted that the phase of $x_\perp$ is $\omega t - \pi/2$, and therefore lags the rf phase by a constant value, $-\pi/2$, independently of the flight angle. Another remarkable consequence of the condition expressed by Eq. (7) is manifested by considering the field distribution of the TM_{110} mode (Fig. 1). Along the orbit in Eq. (8), $E_z = 0$, and the electrons do not extract energy from the input source.[1] Consequently, the beam-loaded quality factor, Q, is equal to the cold cavity Q_0.

It follows from Eq. (8) that the electron deflection in the input cavity reaches a maximum when the flight angle $\theta = \pi$. At this flight angle the transverse position and velocity of the beam centroid are given by

$$x_\perp = i\frac{2\omega_c v_{z0}}{\omega^2} \exp(i\omega t_0) \ , \tag{9}$$

$$v_\perp = -\frac{2\omega_c v_{z0}}{\omega} \exp(i\omega t_0) \ . \tag{10}$$

Thus, if the length of the input cavity is chosen to be equal to $\pi v_{z0}/\omega$ the electron with axial velocity equal to v_{z0} will exit the cavity with the largest possible transverse deflection along its orbit. If one observes the electrons at a fixed point in the input cavity, as time progresses the centroid of the beam is seen to encircle the z-axis.

For the more general case of the orbit in Eq. (6) the transverse deflection of the electron is not necessarily a maximum at $\theta = \pi$. However, for a low-emittance, paraxial beam it is reasonable to take the length of the input cavity to be $\pi v_z/\omega$, where v_z is the mean axial velocity of the beam electrons. The transverse position

and velocity of the electron are now given by

$$x_\perp = x_{\perp 0} + \frac{v_{\perp 0}}{i\omega_c}[\exp(i\pi\omega_c/\omega) - 1]$$

$$+ \frac{\omega_e v_{z0}}{i(\omega - \omega_c)}\exp(i\omega t_0)\left[\frac{2}{\omega} + \frac{\exp(i\pi\omega_c/\omega) - 1}{\omega_c}\right], \qquad (11)$$

$$v_\perp = v_{\perp 0}\exp(i\pi\omega_c/\omega) + \frac{\omega_e v_{z0}}{\omega - \omega_c}[\exp(i\pi\omega_c/\omega) + 1]\exp(i\omega t_0). \qquad (12)$$

III. Passive Cavities

The purpose of the passive cavities in a magnicon is to increase the transverse momentum of the electrons, since the interaction in the output cavity is designed to extract most of the transverse momentum and transfer the energy into the output rf field. To achieve high efficiency in the output cavity, it is necessary to maximize the perpendicular momentum (while avoiding electron reflection) at the end of the deflection system. This generally implies that the pitch angle, $\alpha \equiv \tan^{-1} |v_t|/v_z$ [where $v_t = (v_x^2 + v_y^2)^{1/2}$ is the transverse velocity], exceeds unity.

Although a magnicon may have several passive cavities, the physical principles of their operation are identical. For this reason we consider here a single passive cavity following the input cavity. We further assume that there exists a gap between these cavities, wherein the beam performs gyromotion in the axial magnetic field as it drifts towards the passive cavity. It turns out that the length of the drift region is important for an efficient excitation of the mode. In the first subsection we give an intuitive argument on the role of the drift region, and in the second we examine the field in the passive cavities in the linear regime.

A. Mode excitation

In the case where $\omega_c = 2\omega$, the guiding center of the orbit given by Eqs. (9) and (10) is at $x_{\perp,G} = x_\perp/2$. In the drift region the beam centroid orbit touches the z-axis at a flight angle $\theta_d = \pi/2$, and completes one gyrational motion at $\theta_d = \pi$. Here, $\theta_d = \omega(t - t_0 - \pi/\omega)$ is the flight angle measured in the drift region. The

length of the drift region determines the initial injection conditions for the second cavity. We compare two cases: $\theta_d = \pi$ and $\theta_d = \pi/2$. In the former case the beam enters the passive cavity at the maximum deflection amplitude, while in the latter the beam enters on axis.

(i) $\underline{\theta_d = \pi}$

The initial entrance position and velocity are given by (9) and (10), respectively, with an entrance time $t_1 = t_0 + 2\pi/\omega$ in place of t_0. Let us define the field parameter $\omega'_e = |e|E'_0 \exp(i\phi')/\gamma_0 mc$, where E'_0 is the field amplitude in the passive cavity, in place of E_0, in Eq. (1). The field parameter ω'_e is generally a complex number since there may be a difference in phase–denoted by ϕ'–of the rf fields in the input and passive cavities. The equation of motion of the beam centroid is identical to Eq. (5) except that the coefficient ω_e is now ω'_e. Upon solving the equation of motion for the initial conditions given by Eqs. (9) and (10) we find that

$$x_\perp = \frac{2v_{z0}}{i\omega^2} \left(\omega'_e \sin^2 \frac{\theta}{2} - \omega_e \cos\theta \right) \exp(i\omega t) \quad , \tag{13}$$

where $\theta = \omega(t - t_0 - 2\pi/\omega)$ is the flight angle measured in the passive cavity. Since ω'_e is a complex number the phase of $x_\perp$ given by Eq. (13) is a function of θ except for extreme cases, i.e., when $|\omega_e| \gg |\omega'_e|$ or $|\omega'_e| \gg |\omega_e|$.

The limit $\omega_e \gg |\omega'_e|$ is applicable to the initial build-up stage of the cavity mode. This limit is also useful in accounting for the final equilibrium stage. This is because ω_e carries the information relating to the beam modulation in the input cavity, and, consequently, the term proportional to ω_e acts as a driving term for the oscillations.

8

Making use of the orbit in Eq. (13), $\mathbf{v} \cdot \mathbf{E}$ averaged over $0 \leq \theta \leq \pi$ is found to be zero independently of the field phase. That is, the mode is not driven by the electron motion and the beam deflection obtained in the input cavity is not useful for driving the mode in the passive cavity.

(ii) $\underline{\theta_d = \pi/2}$

We begin by considering the case $\omega_c/\omega = 2$ and an electron starting out on the axis with zero transverse velocity at the entrance to the input cavity. In terms of the entry time into the passive cavity, $t_1 = t_0 + 3\pi/2\omega$, the initial conditions in this case are given by

$$x_\perp = 0 , \tag{14}$$

$$v_\perp = i\frac{2\omega_c v_{z0}}{\omega} \exp(i\omega t_1) . \tag{15}$$

The electrons have been brought to the z-axis through the gyromotion in the drift region, and then injected into the second cavity. With such an injection the beam centroid orbit in the passive cavity is

$$x_\perp = \frac{2v_{z0}}{i\omega^2} \left(\omega_c' \sin^2 \frac{\theta}{2} - \omega_c \sin\theta \right) \exp(i\omega t) , \tag{16}$$

where $\theta = \omega(t - t_1)$ is the flight angle measured in the passive cavity. Note that in Eq. (16), ω_c, which carries the deflection information from the input cavity, is now a coefficient of $\sin\theta$, instead of $\cos\theta$ as in Eq. (13). The beam centroid, which lies on the z-axis initially, reaches a maximum displacement at $\theta = \pi/2$, and then returns to the axis at $\theta = \pi$. Hence, the electric field can be always parallel to the

9

beam propagation direction. The average energy transferred into the field would be nonzero.

The two cases compared above suggest that the optimal length for the drift space is that for which the transit time of the electron is half of a gyroperiod. We may suppose that this is also the case when $\omega_c/\omega \neq 2$ and $x_{\perp 0}, v_{\perp 0} \neq 0$ provided, of course, that $|\omega_c/\omega - 2|$ and $x_{\perp 0}$ and $v_{\perp 0}$ are sufficiently small. For this, more general, case Eq. (16) goes over into

$$
\begin{aligned}
x_\perp \;=\; & x_{\perp 0} - \frac{v_{\perp 0}}{i\omega_c}[\exp(i\pi\omega_c/\omega) + 1] - \frac{v_{\perp 0}}{i\omega_c}\{\exp[i\omega_c(t - t_1)] - 1\}\exp(i\pi\omega_c/\omega) \\[2mm]
& - \frac{v_{z0}\omega_e'}{i(\omega - \omega_c)}\exp(i\omega t) \\[2mm]
& \times \left\{ \frac{1}{\omega} - \left(\frac{1}{\omega} - \frac{1}{\omega_c}\right)\exp[-i\omega(t - t_1)] - \frac{1}{\omega_c}\exp[i(\omega_c - \omega)(t - t_1)] \right\} \\[2mm]
& - \frac{v_{z0}\omega_e}{i(\omega - \omega_c)}\exp(i\omega t)\exp(-i\pi\omega/\omega_c) \\[2mm]
& \times \left\{ 2\left(\frac{1}{\omega} - \frac{1}{\omega_c}\right)\exp[-i\omega(t - t_1)] - \frac{1 + \exp(i\pi\omega_c/\omega)}{\omega_c}\exp[i(\omega_c - \omega)(t - t_1)] \right\},
\end{aligned}
\tag{17}
$$

where $t_1 = t_0 + \pi/\omega + \pi/\omega_c$ is the entry time into the passive cavity.

B.   Gain and Phase Shift

To evaluate the small-signal gain and the phase shift of the beam-loaded passive cavity, it is necessary to solve the wave equation with the source term (i.e., the current density) determined by the solution of the equations of motion, Eq. (17). Following the analysis of Manheimer[6], the current density for a monoenergetic beam of electrons with energy γmc^2 may be written as

$$J_z = -I \int d^2 r_{\perp 0} \, d^3 p_0 \, f(\mathbf{r}_{\perp 0}, \mathbf{p}_0) \, \delta(\gamma_0 - \gamma) \, \delta\{\mathbf{r}_\perp - \tilde{\mathbf{r}}_\perp[t, t_1(\mathbf{r}_{\perp 0}, \mathbf{p}_0, t, z)]\} \quad,$$

where I is the beam current, $\tilde{\mathbf{r}}_\perp$ is the orbit in the $x-y$ plane expressed as a function of time t and the entry time t_1 into the cavity and $f(\mathbf{r}_{\perp 0}, \mathbf{p}_0)$ is the probability density of the initial coordinates $\mathbf{r}_0$ and momenta $\mathbf{p}_0$, subject to the normalization condition

$$\int d^2 r_{\perp 0} \, d^3 p_0 \, f(\mathbf{r}_{\perp 0}, \mathbf{p}_0) \, \delta(\gamma_0 - \gamma) = 1.$$

It is thus necessary to solve the wave equation

$$\left(\nabla^2 - \frac{1}{c^2} \frac{\partial^2}{\partial t^2} \right) A_z = -\frac{4\pi}{c} J_z \quad,$$

with the orbit given by Eq. (17) inserted into the expression for the current density. For an azimuthally symmetric probability density and in the paraxial approximation employed here, the term proportional to $x_{\perp 0}$ in Eq. (17) does not contribute. For such a probability density, the wave equation for the rotating TM_{110} reduces to

$$\left(\frac{\omega^2}{c^2} - k_c^2 \right) \omega_e' = 2\epsilon(\omega^2/c^2)\mathcal{J}, \tag{18}$$

where

$$
\begin{aligned}
\mathcal{J} = & \int d^3 p_0 \, g(\mathbf{p}_0) \, \delta(\gamma_0 - \gamma)(\beta_{z0}/\beta_z) \Bigg\{ \frac{\omega_e'}{1 - \frac{\omega_c}{\omega}} \\
& \times \left[1 - \left(1 - \frac{\omega}{\omega_c}\right) \frac{\sin\frac{\theta_L}{2}}{\frac{\theta_L}{2}} \exp\left(-i\frac{\theta_L}{2}\right) - \frac{\exp[i(\frac{\omega_c}{\omega} - 1)\frac{\theta_L}{2}]}{(\frac{\omega_c}{\omega} - 1)\frac{\omega_c}{\omega}} \frac{\sin(\frac{\omega_c}{\omega} - 1)\frac{\theta_L}{2}}{\frac{\theta_L}{2}} \right] \\
& + \frac{\omega_e}{1 - \frac{\omega_c}{\omega}} \left[2\left(1 - \frac{\omega}{\omega_c}\right) \frac{\sin\frac{\theta_L}{2}}{\frac{\theta_L}{2}} \exp\left(-i\frac{\theta_L}{2}\right) \right. \\
& \left. - \left[1 + \exp\left(i\pi\frac{\omega_c}{\omega}\right) \right] \frac{\exp[i(\frac{\omega_c}{\omega} - 1)\frac{\theta_L}{2}]}{(\frac{\omega_c}{\omega} - 1)\frac{\omega_c}{\omega}} \frac{\sin(\frac{\omega_c}{\omega} - 1)\frac{\theta_L}{2}}{\frac{\theta_L}{2}} \right] \Bigg\}. \tag{19}
\end{aligned}
$$

In writing Eq. (19) it has been assumed that that the probability density $f(\mathbf{r}_{\perp 0}, \mathbf{p}_0)$ is a separable function of $\mathbf{r}_{\perp 0}$ and of $\mathbf{p}_0$; the function $g(\mathbf{p}_0)$ appearing in Eq. (19) is the probability density of the initial momenta $\mathbf{p}_0$. Additionally, $\theta_L = \omega L / v_z$, L is the length of the cavity, $\epsilon = [\beta_z / p_{11} J_2(p_{11})]^2 I / I_A$, $I_A = 1.7 \times 10^4 \gamma \beta_z$ is the Alfvén current and $\beta_z = v_z / c$, with

$$v_z = \int d^3 p_0 \, v_{z0} \, g(\mathbf{p}_0) \, \delta(\gamma_0 - \gamma)$$

being the mean axial velocity.

For a realistic electron beam distribution, the integral in Eq. (19) must be evaluated numerically. In order to obtain some insight into the operation of the magnicon, and to estimate the small-signal gain and phase shift, we shall henceforth limit the discussion to the idealized example of a beam of electrons with no thermal spread, all traveling along the z axis with velocity v_z, and $\omega_c / \omega = 2$. In this case, upon evaluating the integral in Eq. (19) and inserting the resulting expression in Eq. (18), one obtains

$$\left[\frac{\omega(\omega + i c k_c / Q)}{c^2} - k_c^2 \right] \omega_e' = -2\epsilon(\omega^2 / c^2)(\alpha_e \omega_e' - 2\alpha_o \omega_e) \; , \qquad (20)$$

where $\alpha_e = 1 - \sin\theta_L / \theta_L$ and $\alpha_o = (1 - \cos\theta_L)/\theta_L$ are parameters depending on the flight angle θ_L in the passive cavity. In writing Eq. (20) we have introduced damping of the mode through the cavity quality factor Q, where the damping rate is given by $\omega / 2Q$.

Upon neglecting the term associated with the Q and that proportional to α_o, Eq. (20) becomes identical to the dispersion relation for the input cavity. Since the

coefficients of this dispersion relation are real, the mode is neutral; i.e., it is neither damped nor unstable. This is consistent with the fact, alluded to in the paragraph following Eq. (8), that the electrons do not exchange energy with the field in the input cavity.

From Eq. (20) the resonant frequency of the undriven cavity, which is modified by the beam loading, is given by

$$\omega \approx ck_c(1 - \epsilon\alpha_e).\tag{21}$$

At this frequency, the maximum gain per passive cavity is, from Eq. (20), given by

$$|\omega'_e/\omega_e| \approx \left[\frac{2\beta_z}{p_{11}J_2(p_{11})}\right]^2 \frac{QI}{I_A}\alpha_0.\tag{22}$$

A 200 A, 1/2 MV electron beam will be employed in the magnicon experiment at the Naval Research Laboratory, which will operate in the X-band (11.4 GHz) with a C-band (5.7 GHz) drive.[4] For these parameters, a power gain of 10 dB is obtained for $Q \approx 500$. The corresponding relative shift in the cold cavity frequency is about 1/2 %. In a magnicon employing a series of passive cavities to accomplish high amplification, the total gain is simply the product of the gain of the individual cavities.[6]

Returning to the orbit in Eq. (16), the deflection at $\theta = \pi$ is given by

$$x_\perp \simeq i\frac{2\omega'_e v_z}{\omega^2} \exp[i\omega t_1] \ ,\tag{23}$$

which is an identical deflection pattern as obtained in the input cavity, Eq. (9), except that the deflection is now amplified a factor of $|\omega'_e/\omega_e|$. In general, a sequence of passive cavities may be required in order to ensure that the final pitch angle α exceeds unity.

IV. Output Cavity

The output cavity of a magnicon employs a TM mode whose phase advances synchronously with the frequency of the drive. Additionally, the interaction in the output cavity is based on the first harmonic of the cyclotron resonance in the axial magnetic field. The preferred choice for the mode is the TM_{m10}, corresponding to an rf field with no axial variation in the cavity, and with a radial variation characterized by the Bessel function of order 1. The index m, which indicates the azimuthal variation of the mode, is chosen to produce the proper phase synchronism with the gyrating electron beam. In practice, this means that for a particular choice of m, the output cavity must operate in the mth harmonic of the drive frequency, as explained in the following. For a first harmonic (of the drive frequency) device, $m = 1$, and the interaction is with a rotating TM_{110} mode. However, in this case, the magnetic field must be reduced to approximately half the magnetic field in the deflection cavities. This is an unfavorable magnetic field configuration for a high-α electron beam.

Operation at the second harmonic of the drive frequency, using the TM_{210} mode, requires a magnetic field that is approximately flat throughout the passive and output cavities. (Actually, the optimum magnetic field in the output cavity is lower than the gyroresonant value at the initial beam energy to compensate for the effect of energy extraction from the beam.) Still higher harmonic operation may be possible, employing TM_{m10} modes with $m > 2$, and taking advantage of the increase in the beam α as the magnetic field is ramped up to the value resonant with the

14

higher frequency in the output cavity. However, there is an overall constraint on the maximum beam α that may be achieved without reflecting the electrons, so that the maximum deflection may be no higher in this case than in the preceding case. Additionally, the coupling to higher harmonics is generally weaker, and may require a longer interaction length.

We note in passing that the problem with oscillations in unwanted modes seems to be not as important as in gyrotrons, since the effectively "super-bunched" scanning beam will induce mode-locking.

Description of the interaction dynamics in the output cavity generally requires a numerical approach. In this section, as a prelude to future numerical efforts, we show that such harmonic operation is possible. For this purpose we use the zeroth order electron orbit with respect to the harmonic modes.

(i) Second Harmonic $(\omega_c = 2\omega)$

Upon neglecting the shift in the gyro-frequency due to the energy loss during interaction we may assume that the magnetic field strength has no discontinuity between the deflection system and the output cavity. We may take the initial conditions for the beam centroid orbit in the output cavity as

$$x_\perp = ix_0 \exp(i\omega t_0), \tag{24}$$

$$v_\perp = -\omega x_0 \exp(i\omega t_0), \tag{25}$$

where x_0 is a constant, and t_0 is the time when a certain section of the beam centroid enters the cavity. Neglecting the rf field, the electron motion for $\omega_c = 2\omega$ with these

15

initial conditions is given by

$$x_\perp = ix_0 \exp(i\omega t) \cos\theta.$$

Note that the phase rotates with an angular frequency ω, and the amplitude of the motion depends only on the flight angle $\theta = \omega(t - t_0)$. Figure 2(a) shows the orbit with respect to the rotating TM_{210} mode of frequency 2ω (for which the angular rotation velocity is ω). It is seen that the beam centroid remains in the proper phase relationship for continuous deceleration by the electric field.

(ii) <u>Third Harmonic $(\omega_c = 3\omega)$</u>

Third harmonic operation requires that the magnetic field in the output cavity be approximately 3/2 that in the deflection cavities. It is reasonable to assume that the transition in the magnetic field between the deflection system and the output cavity may be made sufficiently slow to fulfill the requirements for adiabatic electron motion. In this case, the magnitude of the electron transverse coordinate and velocity at the entrance to the output cavity may be estimated from the conservation of canonical angular momentum, $P_\phi \equiv \gamma m r v_\phi - |e| r A_\phi / c$, and the magnetic moment $\mu \equiv v_t^2 / 2B_0$. Here, v_ϕ is the azimuthal velocity, $v_t = (v_x^2 + v_y^2)^{1/2}$ is the velocity transverse to the guide field B_0, the latter being represented by the vector potential $A_\phi = rB_0/2$. With the initial coordinate and velocity given by Eqs. (24) and (25), the corresponding quantities at the entrance to the output cavity are given by:

$$x_\perp = i(2/3)^{1/2} x_0 \exp(i\phi_x) \ ,$$

$$v_\perp = -(3/2)^{1/2} \omega x_0 \exp(i\phi_v) \ ,$$

16

where ϕ_x and ϕ_v are arbitrary constants, determined by the precise motion of the electron through the transition region. For $\omega_c = 3\omega$, these initial conditions define a gyroradius equal to $x_0/2$. The orbit is given by

$$x_\perp = i\sqrt{\frac{1}{6}}x_0 \left\{ 2\exp(-i\theta) \left[\exp(i\phi_x - i\phi_v) - \frac{1}{2} \right] + \exp(2i\theta) \right\} \exp[i(\phi_v - \omega t_0)] \exp(i\omega t).$$

$$(26)$$

Figure 2(b) shows the orbit with respect to TM_{310} mode of frequency 3ω for the case where $\phi_x - \phi_v$ is a multiple of 2π . The angular rotation velocity of the mode is again ω. Comparing with the case of second harmonic operation, it is seen that a portion of the beam centroid path extends into regions of unfavorable field direction. This suggests that the coupling may be weaker, and as we move up to even higher harmonics, the coupling is further reduced.

V. Conclusion

The electron beam deflection system in a magnetic-field-immersed magnicon has been analyzed. The electrons are injected into the input cavity with a small input signal, and deflected transversely. Deflection is achieved through the rotating magnetic field of the cavity-resonant TM_{110} mode. For the case in which the gyrofrequency in the guide field is twice the signal frequency, the electrons maintain a constant phase relative to the rf mode through the input cavity. Maximum deflection is obtained when the beam transit time through the input cavity is half of the rf period.

For the efficiency of energy conversion to be high, a beam α of order unity or greater is required since a magnicon extracts only the transverse electron momentum. The deflection that is obtained in a single input cavity will not fulfill this requirement unless the input power is extremely large. In order to enhance the ratio of the output to input power (i.e., the gain), use of passive cavities has been considered. Passive cavities are assumed to be immersed in the same guide magnetic field as the input cavity. It has been noted that the gap spacing between cavities is important. Optimal excitation of modes in the passive cavities is achieved when the beam transit time through a passive cavity is half of an rf period and when the transit time in the gap between passive cavities is half of a gyroperiod. The wave equation for the resonant mode in the passive cavities is analyzed and an expression for the gain is obtained. A major simplifying assumption of the analysis presented is that the electron energy is a constant in a passive cavity. In practice this should

be a good approximation except perhaps for the last sequence of passive cavities, which produces an $\alpha > 1$.

We have considered the case where the gyrofrequency in the passive cavities is twice the drive frequency and the gyrofrequency in the output cavity is approximately equal to the output frequency. Consequently, second (or higher) harmonic (of the drive frequency) operation appears desirable.

Acknowledgment

References

[1] M. M. Karliner, E. V. Kozyrev, I. G. Makarov, O. A. Nezhevenko, G. N. Ostreiko, B. Z. Persov and G. V. Serdobintsev,"The Magnicon–An Advanced Version of the Gyrocon," *Nucl. Instrum. Methods Phys. Res.*, vol. A269, pp. 459-473, 1988.

[2] R. S. Symons and H. R. Jory, "Cyclotron Resonance Devices," in *Advances in Electronics and Electron Physics*, vol. 55, edited by L. Marton and C. Marton (Academic Press, New York, 1981), pp. 1-75.

[3] O. Nezhevenko, "The Magnicon: A New rf Power Source for Accelerators," in *Proc. 1991 IEEE Particle Accelerator Conf.*, in press.

[4] S. H. Gold, B. Hafizi, W. M. Manheimer and C. A. Sullivan, "Design of a High-Perveance, Field-Immersed Magnicon," in *Conf. Digest–Sixteenth Int. Conf. Infrared and Millimeter Waves*, in press.

[5] N. C. Jaitly, M. Coleman, S. Eckhouse, A. Ramrus, S. H. Gold, R. B. McCowan and C. A. Sullivan, "1 MV Long Pulse Generator with Low Ripple and Low Droop," in *Proc. Eighth IEEE Pulsed Power Conf.*, in press.

[6] W. M. Manheimer, "Theory and Conceptual Design of a High-Power Highly Efficient Magnicon at 10 and 20 GHZ," *IEEE Trans. Plasma Sci.*, vol. PS-18, pp. 632-645, 1990.
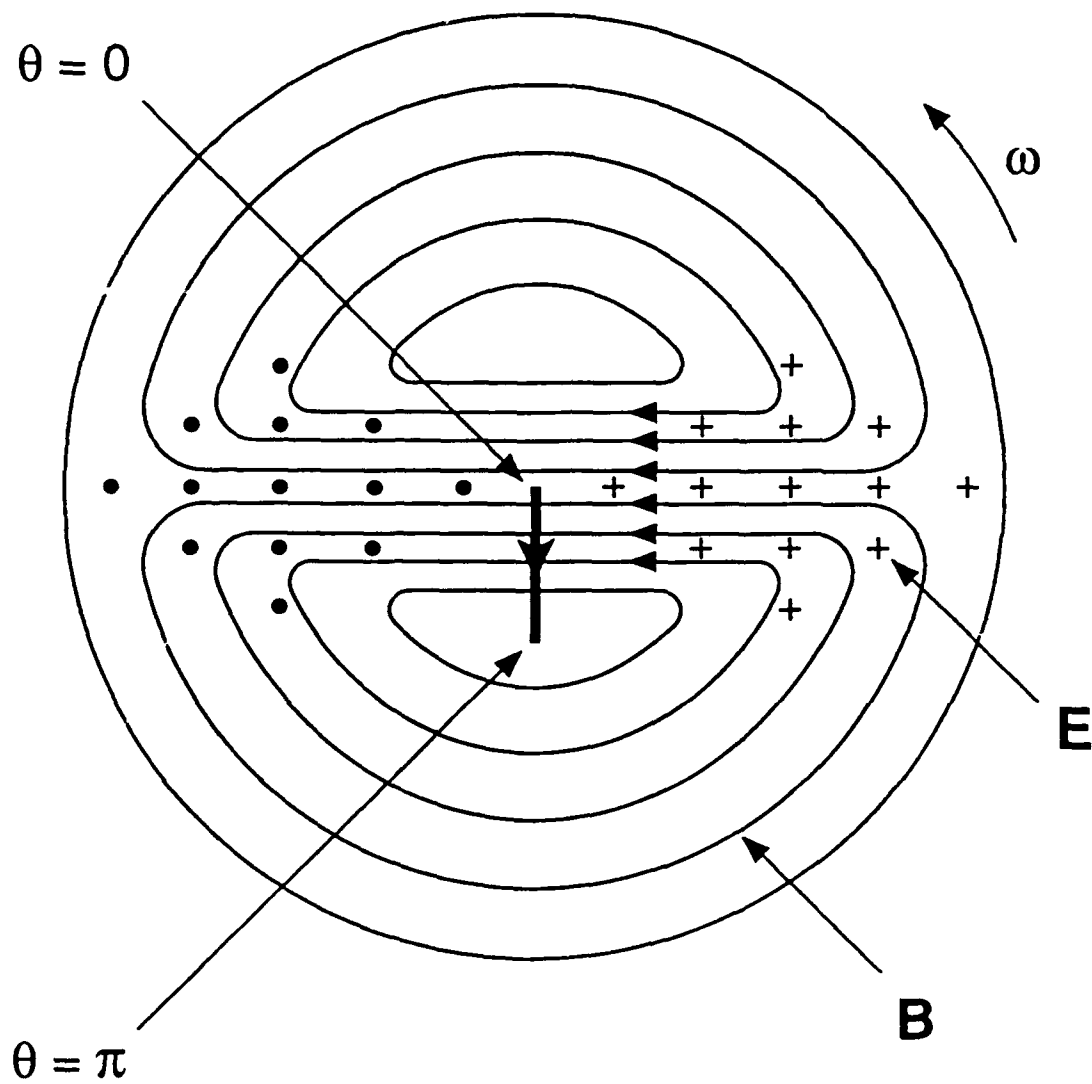
Fig. 1 — Beam centroid in the input cavity relative to the rotating cavity mode. The path, shown by a heavy line, lies where $E_z = 0$. The electric field is shown by "+" and "●," and the magnetic field is indicated by solid curves. The flight angle is denoted by θ.
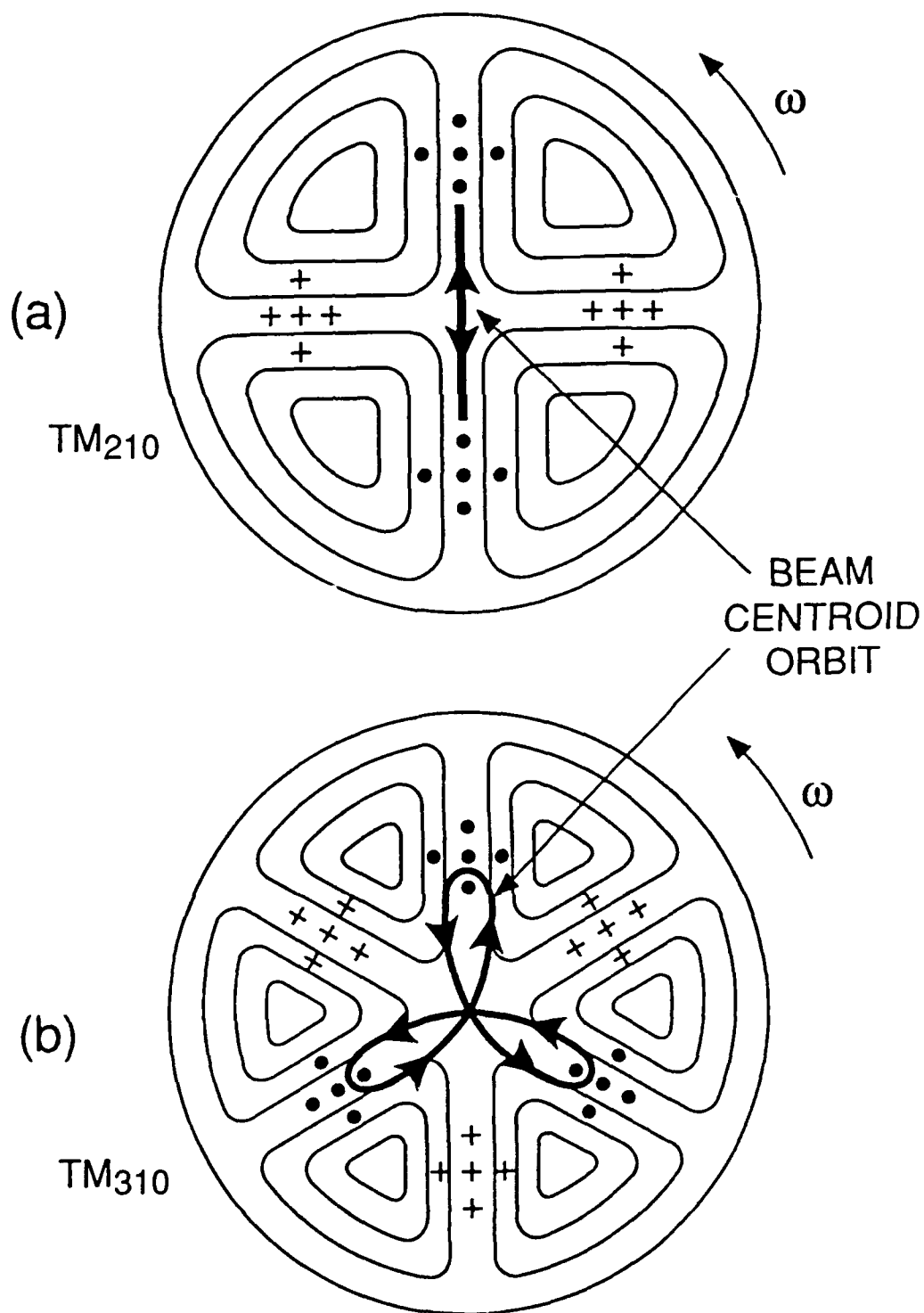
Fig. 2 — Zeroth order beam centroid in the output cavity relative to rotating cavity modes. (a) Beam centroid relative to TM_{210} mode at second harmonic frequency. (b) Beam centroid relative to TM_{310} mode at third harmonic frequency.